Physica A 633 (2024) 129394

Contents lists available at ScienceDirect

Physica A

journal homepage: www.elsevier.com/locate/physa

Modeling pedestrian single-file movement: Extending the interaction to the follower

Rudina Subaih [a,b,*], Antoine Tordeux [b]

[a] Institute for Advanced Simulation, Forschungszentrum, Jülich, 52425, Germany
[b] School for Mechanical Engineering and Safety Engineering, University of Wuppertal, Wuppertal, 42119, Germany

ARTICLE INFO

Keywords:
Pedestrian dynamics
Single-file movement
Microscopic model
Least squares parameter estimate
Fundamental diagram
Stop-and-go waves

ABSTRACT

This article proposes a new microscopic speed model for one-dimensional pedestrian movement. Most existing modeling approaches consider only the distance and relative speed between a pedestrian and the person in front resulting in totally asymmetric interaction models. However, the distance with the pedestrian behind may also influence the behavior of a pedestrian. Based on this assumption, we elaborate a new asymmetric microscopic model considering the relative distances with the nearest neighbors behind and ahead using a fine-tuning asymmetry parameter. We analyze the stability of the new model and calibrate the parameters using two different single-file movement datasets. The numerical simulation results show that the new model has fewer backward movements and pedestrian overlaps than the totally asymmetric model making the stop-and-go waves in crowded situations more realistic. Furthermore, the proposed fine-tuned model better describes the fundamental diagram and its scattering.

1. Introduction

Modeling pedestrian dynamics is essential to organizing safe and efficient crowded events. For instance, the models can be used to develop simulation software and assist in decision-making, risk management, and policy development for large pedestrian events. Various models have been developed to describe single-file pedestrian movements [1–7]. Generally speaking, pedestrian models are mainly categorized as microscopic [7–14] and macroscopic [15–20] based on the motion characteristics investigated (see [21] for review). Macroscopic models describe the aggregate characteristics of crowds, while microscopic models focus on the movement of individual pedestrians. Furthermore, the models can be discrete, such as microscopic cellular automata and macroscopic lattice models, or continuous, using systems of differential equations. The cellular automata models are random by nature, whereas in continuous approaches stochasticity can be introduced through adding noise to the dynamics. All these models are subject to many modeling assumptions that describe the way people move and interact with their environment. Several parameters and variables have been introduced in microscopic models to describe pedestrian interaction behaviors in single-file motions. In most cases, the models are totally asymmetric, i.e., the interaction model is only based on the distance to the nearest pedestrian in front and the speed of that pedestrian.

In this paper, we propose a new microscopic stochastic model to describe pedestrians' single-file movement. The originality of the approach lies in the interaction model, which also depends on the distance to the pedestrian behind. The model is inspired by previous statistical investigations [22] and empirical observations of coordination phenomena in single-file motion [23]. A parameter fine-tuning the relative distance to the neighbors in front and behind is applied. To study the model's behavior, we analyze the linear

* Corresponding author at: Institute for Advanced Simulation, Forschungszentrum, Jülich, 52425, Germany.
E-mail addresses: r.subaih@fz-juelich.de (R. Subaih), tordeux@uni-wuppertal.de (A. Tordeux).

https://doi.org/10.1016/j.physa.2023.129394
Received 10 July 2023; Received in revised form 30 October 2023
Available online 20 November 2023

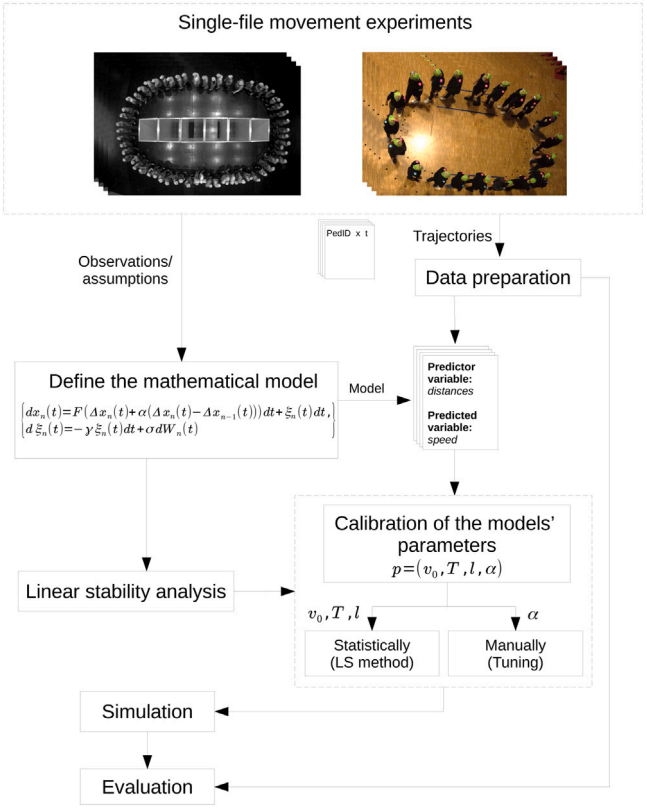

Fig. 1. Key methodological milestones in the process of defining and evaluating the proposed pedestrian speed model.

stability focusing on the role of the weight of the relative distances. We then calibrate the parameters of the deterministic speed model using two single-file movement datasets and different methods: statistically by least squares and empirically by simulation. Finally, we numerically investigate the movement of pedestrians in one-dimensional space and compare the simulation results with the totally asymmetric model and the real data. The simulation analysis focuses on space–time trajectories and fundamental diagrams (headway-speed relation). A summary of our methodology is presented in Fig. 1. The results show that the new model improves the description of the fundamental diagram scattering and stop-and-go waves, making the simulation results more realistic.

The rest of the paper is structured as follows: we review and discuss the literature on pedestrian single-file movement models in Section 2. In Section 3, the microscopic speed model considering the symmetric interaction is defined. Then, in Section 4, we analyze the linear stability of the deterministic model to investigate theoretically the behavior of the proposed first-order speed model. The calibration of the model's parameters is presented in Section 5. In Section 6, the simulation results are presented and discussed. Finally, in Section 7, we summarize the content of the paper.

2. Related work

To better understand pedestrian dynamics in complex movement systems, many researchers investigate and model pedestrian behavior in one-dimensional space. Many single-file movement experiments (pedestrians walking in a single line or queue) have been performed to observe and analyze the factors that influence pedestrians' speeds, e.g., recent experiments performed in Germany, Palestine, and Japan [24–26]. Further pedestrian trajectories from single-file experiments are available online.[1] The single-file experiments provide a basic analysis of pedestrian dynamics, focusing on the fundamental relationship between speed and distance from neighbors. Various models based on the experiments have been developed in the literature to reproduce the observed trajectories as closely as possible. The observation of the experiments inspired, for instance, Chraibi et al. [7] to introduce the velocity-dependent volume exclusion of pedestrians into the force-based model. The authors observed from the experiments that pedestrians' speed is influenced by their shoulder rotation while avoiding others, leading them to conclude that using a dynamic agent shape would be more effective than a static one. This results in the improvement of the simulation of pedestrians in crowds. Another study by Cordes et al. [1] applies the concept of time-to-collision (TTC) to model single-file pedestrian movement.

[1] Pedestrian dynamics data archive: https://ped.fz-juelich.de/da/doku.php

The authors assume that the TTC quantifies the distance to a collision (between pedestrians) by combining spatial distances and velocities. That aims to give rise to a new class of models that represent the interactions among pedestrians by evolving TTC.

Several pedestrian models were proposed, drawing inspiration from other models. For instance, using car-following models to describe the single-file movement, Lemercier et al. [4] elaborated a pedestrian interaction model. The model focuses on the following behavior of pedestrians walking in corridors or queues. The authors verified the Aw et al. [27] road traffic model in pedestrian traffic and formulated a new model of interactions adapted to crowd simulation. Kuang et al. propose an extended optimal velocity model [5]. This model simulates the single-file movement in high density considering the interaction forces (repulsive and attractive forces) between pedestrians. Other pedestrian single-file models are derived from two-dimensional force-based models, such as [3,6]. The issues of agent overlapping and oscillation in the social force model (as mentioned in [8,28–31]) can be linked, in a one-dimensional case, to the limitations of the optimal velocity car-following model. To prevent backward movements, oscillations, and collisions, the optimal velocity (OV) model requires fine-tuning of the parameters [32]. Such unrealistic simulations' shortcomings of single-file behavior can be addressed using extended models.

The distance behind is introduced in considerable traffic system models (vehicle models) [33–38]. For example, Ge et al. [37] propose an extended car-following model by introducing the backward-looking effect. The model considers several vehicles ahead and one behind in a single lane. The simulation of the space–time evolution of the car headways shows that the model suppressed the traffic jam. Additionally, the findings of the linear stability analysis demonstrate that taking into account the backward-looking effect leads to the stabilization of the traffic system. Minghui Ma et al. [33] also propose an improved car-following model (cars driven in a single-file setup) by considering the backward-looking behavior and motion information of multiple vehicles. The drivers usually look behind while driving to avoid collisions with other vehicles. The simulation results show an efficient improvement in the avoidance of traffic congestion and enhance the stability of the traffic flow in comparison to the models that include only the distance in front. In pedestrian dynamics, Rio et al. [23] investigate the visual control of pedestrians following behavior. Using experimental investigations, the authors study how pedestrians adjust their walking speed when following a leader, based on the visual information provided by the leader's movements. The study involved experiments with pairs of participants walking in a straight line, with one person leading and the other following. The results show that the follower's walking speed is influenced by the leader's speed and visual cues, including the leader's head movements and changes in the walking direction. Considering the findings of Rio et al. we assume that there is coordination between the distances of pedestrians and their neighbors in the crowd, which influences the individual speeds of pedestrians.

In summary, existing pedestrian single-file movement models are systematically totally asymmetric and can encounter problems with overlapping and backward motion. Such difficulties are well-known for car-following models and can be overcome by extending the interaction to the agent behind [33,39], leading to stability improvement and better collective coordination. Besides, collective coordination is observed in pedestrian single-file movements [23]. Furthermore, recent statistical analysis using feed-forward neural networks devoid of modeling bias shows that the distance behind improves the speed prediction [22]. These statements motivate us to extend a stochastic pedestrian single-file model by incorporating the distance to the pedestrian behind. Including the distance behind reduces unrealistic pedestrian overlaps and backward movements, which are observed in totally asymmetric models under high-density conditions. The model is a scaled-down version used to demonstrate specific aspects of the original system with fewer influential factors and in a simplified way.

3. Proposed model

We consider a single-file movement of pedestrians in continuous time on a uni-dimensional space of length L with periodic boundary conditions. The pedestrians initially ordered by their indexes $n = 1, 2, \dots, N$ and assume that the follower and predecessor of the nth pedestrian are the $(n-1)$th and $(n+1)$th pedestrians at any time, respectively. Due to the periodic boundary conditions, the predecessor of the last pedestrian is the first agent and the follower of the first pedestrian is the last one as illustrated in Fig. 2. The x-axis position of a pedestrian n at time t is denoted as $x_n(t)$. To calculate the distances between the consecutive pedestrians, we subtract the positions as:

$$\begin{cases} \Delta x_n(t) = x_{n+1}(t) - x_n(t), & n = 1, \dots, N-1, \\ \Delta x_N(t) = L + x_1(t) - x_N(t). \end{cases} \tag{1}$$

In the proposed pedestrian single-file model, we assume that pedestrians can feel how close (the distance) the person behind is, which affects how they behave and extends the interaction. For the nth pedestrian, the model is given by the following stochastic differential equation:

$$\begin{cases} dx_n(t) = F\big(\Delta x_n(t) + \alpha(\Delta x_n(t) - \Delta x_{n-1}(t))\big)dt + \xi_n(t)dt, \\ d\xi_n(t) = -\gamma\xi_n(t)dt + \sigma dW_n(t). \end{cases} \tag{2}$$

Here the speed of a pedestrian is an OV function F coupled to a stochastic noise provided by the Ornstein–Uhlenbeck process with rate $\gamma > 0$ and volatility $\sigma \in \mathbb{R}$, and $W_n(t)$ being a Wiener process. The Ornstein–Uhlenbeck process is used to enhance the smoothness of noise evolution and make the noise more realistic than white noise in speed-based models (see [2] for a more detailed description). The OV function is assumed positive, increasing, and bounded by the maximal desired speed.

In contrast to the totally asymmetric model [2], the OV function depends on a weighted average between the distance to the predecessor $\Delta x_n(t)$ and the distance to the follower $\Delta x_{n-1}(t)$, adjusted by a dimensionless, fine-tuning asymmetry parameter $\alpha \in \mathbb{R}$. The totally asymmetric model is restored if $\alpha = 0$. Conversely, the speed function only depends on the distance to the follower if

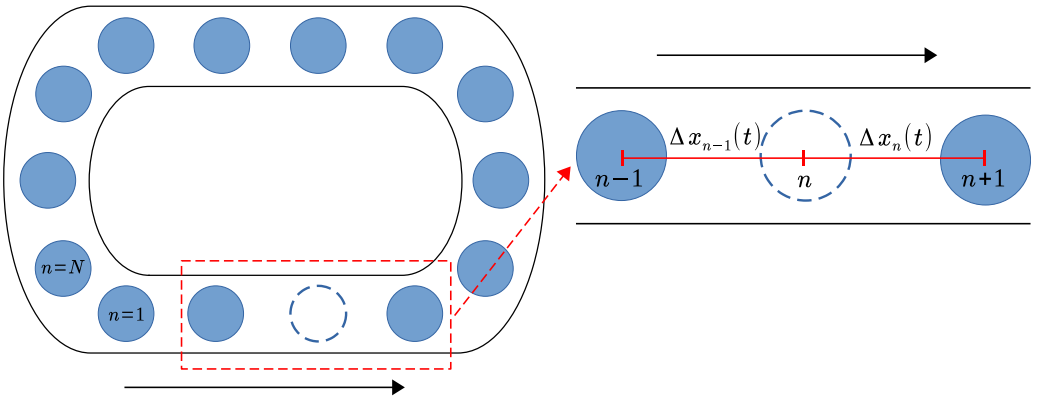

Fig. 2. Scheme of the system with periodic boundary conditions. $\Delta x_n(t)$ is the distance of the pedestrian n to the predecessor at time t, while $\Delta x_{n-1}(t)$ is the distance to the follower.

$\alpha = -1$, whereas it is symmetric and depends on the arithmetic mean of the distances to the follower and the predecessor if $\alpha = -1/2$. Intuitively, the cases $\alpha > 0$ lead to homogenization dynamics, as a large distance ahead and a small distance behind results in a higher speed, while a small distance ahead and a large distance behind results in a lower speed and inversely.

The OV function $F : \mathbb{R} \mapsto \mathbb{R}^+$ includes classical parameters related to the pedestrian characteristics and behaviors, such as the desired speed $v_0 > 0$, the desired time gap $T > 0$, and the pedestrian size (circle width) $\ell > 0$. A typical OV function is the following bounded linear function:

$$F(x) = \min\left\{ v_0, \frac{x_n(t) - \ell}{T} \right\} \tag{3}$$

that we approximate using the smoothed Log-Sum-Exp function [40] given by:

$$F_\varepsilon(x) = -\varepsilon \log\left(\exp\left(-\frac{v_0}{\varepsilon} \right) + \exp\left(-\frac{x_n(t) - \ell}{T\varepsilon} \right) \right), \qquad \text{as} \quad \varepsilon \to 0. \tag{4}$$

In the following, we set the speed smoothing ε to 0.01 m/s.

4. Linear stability analysis

We first examine the linear stability of the deterministic first-order model (Eq. (2)) to determine possible values of parameters. Applying stability analysis allows us to investigate the behavior of the proposed first-order deterministic model (Eq. (2)). Therefore, we need to determine the behavior of a solution to the differential equation as follows.

In general, suppose a linear differential equation given by the form:

$$f'(t) = af(t), \qquad \text{where } t \in [0, \infty) \text{ and } a \in \mathbb{R} \tag{5}$$

The general solution of Eq. (5) above is:

$$f(t) = be^{at}, \tag{6}$$

with $b = f(0)$. Indeed, we have in this case:

$$f'(t) = abe^{at} = af(t). \tag{7}$$

So, $f'(t)$ depends on the value of the constant a. It converges if and only if the value of a is non-positive, i.e.,

$$a < 0, \tag{8}$$

otherwise the system will collapse.

Focusing on the interactive part of the model, the single-file dynamics for the nth pedestrian is given by:

$$\begin{aligned} \dot{x}_n(t) &= \frac{1}{T}(\Delta x_n(t) + \alpha(\Delta x_n(t) - \Delta x_{n-1}(t))) \\ &= \frac{1}{T}((1+\alpha)\Delta x_n(t) - \alpha \Delta x_{n-1}(t)). \end{aligned} \tag{9}$$

Table 1
Table summarizing CroMa and BaSiGo datasets used for parameter calibration and model validation.

Experiment	Location, date	Geometry length [m]	Number of participants	Frame-rate [fps]	Investigation	Pedestrian identification across runs
CroMa	Düsseldorf, Germany (2021)	14.97	$N = 8, 16, 20, 24, 32, 36, 40$	25	Gender factor (mixed)	✓
BaSiGo	Düsseldorf, Germany (2013)	26.84	$N = 15, 30, 47, 52, 55, 59$	16	Congested dynamic	

By substituting $\Delta x_n(t) = x_{n+1}(t) - x_n(t)$ and $\Delta x_{n-1}(t) = x_n(t) - x_{n-1}(t)$ into Eq. (9) we obtain:

$$\begin{aligned}\dot{x}_n(t) &= \frac{1}{T}((1+\alpha)x_{n+1} - (1+2\alpha)x_n + \alpha x_{n-1}) \\ &= \frac{1}{T}(1+\alpha)x_{n+1} - \frac{1}{T}(1+2\alpha)x_n + \frac{1}{T}\alpha x_{n-1} \\ &= -\frac{1}{T}(1+2\alpha)x_n + \frac{1}{T}((1+\alpha)x_{n+1} + \alpha x_{n-1}) \\ &= a x_n + C(x_{n+1}, x_{n-1})\ dt\end{aligned} \tag{10}$$

with:

$$a = -\frac{1}{T}(1+2\alpha), \tag{11}$$

and:

$$C(x_{n+1}, x_{n-1}) = \frac{1}{T}((1+\alpha)x_{n+1} + \alpha x_{n-1}). \tag{12}$$

Then the system will be stable if the stability condition $a < 0$ is satisfied (see condition (8)), which is given by

$$-\frac{1}{T}(1+2\alpha) < 0,$$

which is equivalent to:

$$\alpha > -1/2, \tag{13}$$

as $T > 0$.

Interestingly, the critical value is:

$$\alpha_C = -1/2 \tag{14}$$

corresponds to a symmetric case where the distance in the OV function is the arithmetic mean of the distances to the nearest neighbors in front and behind. Setting $\alpha > -1/2$ makes the weight for the distance ahead higher than the weight for the distance behind. Therefore, the following model is only stable if the interaction model is asymmetric, giving more importance to the distance to the neighbor in front.

5. Parameters calibration

5.1. Single-file movement datasets and data preparation

Two different experimental datasets are used to statistically estimate the parameters of the model and for comparison with the simulation results. The first data sample is the one-dimensional dataset of Paetzke et al. [24]. Several experiments were conducted in Düsseldorf, Germany in 2021 to study the influence of gender on pedestrian movement. The pedestrians were instructed to move in an oval corridor one after the other without haste and overtaking (see Fig. 3). We select the mixed alternating experiment for the parameters' calibration. The data includes different experimental runs with a pedestrian number varying between $N = 8, 16, 20, 24, 32, 36, 40$. That ensures obtaining different ranges of variation of distances between pedestrians, and speeds. The data of each pedestrian in the different experimental runs are collected and labeled with pedestrian ID (unique number). This data will be used to estimate individually the model's parameters (see Section 5.2). For more details on the experiment, refer to the article [24].

The second experiment dataset used for parameter calibration and validation of the numerical simulation is the single-file movement dataset by Ziemer et al. [41]. The experiment (see Fig. 4), conducted in Germany within the project BaSiGo, focuses on the analysis of pedestrians' dynamic moving in an oval system with periodic boundary conditions. We use in the following the data of the experiments with $N = 15, 30, 47, 52, 55, 59$ participants. Evaluating the model with two different datasets will ensure that the model is reliable and generalizes well to new data. Table 1 summarizes the main information about the experiments.

Fig. 3. Overhead view of the CroMa single-file movement experiment run $N = 20$.

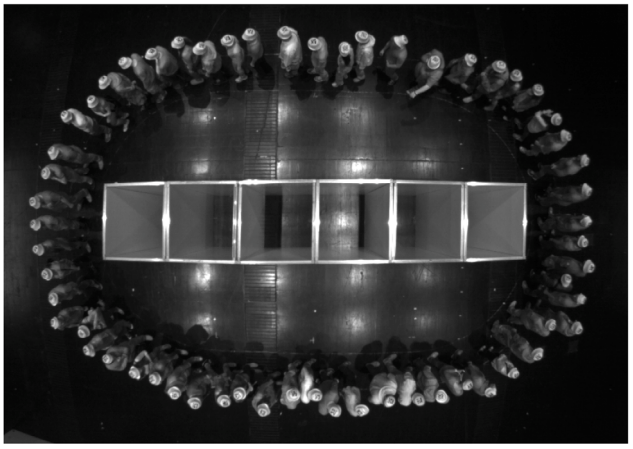

Fig. 4. Overhead view of the BaSiGo single-file movement experiment run $N = 59$.

The trajectory data from the experiments is used to calculate the pedestrian positions $x_n(t)$, the speed $v_n(t)$, and the distance in the front $\Delta x_n(t)$ and behind $\Delta x_{n-1}(t)$. Here is the equation of the pedestrian's speed:

$$v_n(t) = \frac{x_n(t + \Delta t/2) - x_n(t - \Delta t/2)}{\Delta t}, \tag{15}$$

where Δt short time interval around t (10 frames, i.e., 0.4 s).

5.2. Nonlinear least squares estimates of the parameters

The calibration of the proposed model (2) is necessary for making quantitative predictions. To achieve this, we need to adjust the models' parameters to fit the different samples of experimental data. We use the nonlinear least squares method to estimate the parameters $p = (v_0, T, \ell, \alpha)$ related to the deterministic part of the model (see (2) and (4)). The non-linear speed model reads as follows:

$$M_p(\Delta x_n, \Delta x_{n-1}) = F_{v_0,T,\ell}\big(\Delta x_n + \alpha(\Delta x_n - \Delta x_{n-1})\big), \tag{16}$$

with F the smoothed optimal velocity function given in (4). The regression is nonlinear since the OV function is sigmoidal. Then, using an experimental sample of K observations of individual speed and distances in front and behind $(s_k, \Delta x_k, \Delta x_k^0)$ where $k = 1, \dots, K$, we estimate the parameters p by minimizing the difference to the square between the observed speeds and the model

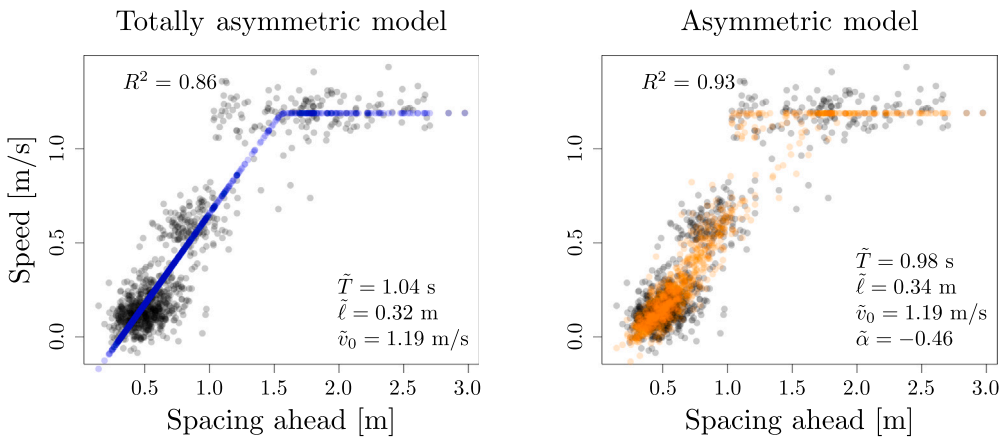

Fig. 5. Global estimates of the model's parameters (without noise) using nonlinear least squares. The scatter plots of the fundamental diagram for the BaSiGo experimental dataset and the predictions of the totally asymmetric model (left panel) and the asymmetric model (right panel) are presented. The parameters' estimates (T, ℓ, v_0) of the optimal velocity are close to each other for both models. The asymmetric model reproduces the variability of the fundamental diagram and improves the prediction. Note that only 16% of the data samples are shown in the scatter plots to improve the readability of the figure.

predictions:

$$\tilde{p} = \arg\min_{p} \sum_{k=1}^{K} \left(s_k - M_p(\Delta x_k, \Delta x_k^0)\right)^2. \tag{17}$$

The model residuals are the variables:

$$R_k(\tilde{p}) = s_k - M_{\tilde{p}}(\Delta x_k, \Delta x_k^0) \tag{18}$$

The least squares estimates minimize the sum of squared residuals. In the following sections, we begin by presenting the global parameter estimates over the full data samples, followed by individual estimates calculated for each pedestrian. Subsequently, we delve into a detailed discussion of the estimates for α.

5.2.1. Global parameter estimates

Fig. 5 illustrates the global parameter estimations over the full samples for the totally asymmetric model (with initialized $\alpha = 0$) and the proposed asymmetric model (with estimated α) without noise (presenting the deterministic part of the model). Note that for the initial model with $\alpha = 0$, the speed solely depends on the distance in front. The optimal velocity function appears directly (see Eq. (3) and Fig. 5, left panel). On the other hand, the extended speed model depends on the distances in front and behind, allowing to reproduction of a certain variability even in the deterministic framework (see Fig. 5, right panel). The results show that the estimates of the parameters (T, ℓ, v_0) for the optimal velocity function are equivalent to the totally asymmetric and asymmetric models. The estimates for T are 1.04 s and 0.98 s, and for ℓ are 0.32 m and 0.34 m for totally asymmetric and asymmetric models, respectively. While, the desired velocity, v_0, is 1.19 m/s for both models. Therefore, the model extension with the fine-tuning parameter α does not affect the shape of the fundamental (distance-speed) relationship. We note that the estimated value of $\alpha = -0.46$ is negative and close to the critical stability condition ($\alpha_C = -1/2$).

Furthermore, we observe that the asymmetric model with an estimated α has the highest R^2 value ($R^2 = 0.93$) compared to the totally asymmetric model ($R^2 = 0.86$). Indeed, it also recovers part of the variability of the distance-speed relationship. The proposed model captures the variability of the data points better than the totally asymmetric model. However, this is not surprising as the asymmetric model has one more parameter.

The distributions of the residuals of both models are compact as shown in Fig. 6. This means that the least squares estimates are close to the maximum likelihood estimates. The distribution for the asymmetric model is slightly more concentrated with a lower standard deviation. The standard deviation of the residual is approximately 0.15 m/s for the totally asymmetric model while it is 0.11 m/s for the new asymmetric model. A Fisher test for equality of the variance allows rejecting the equality hypothesis without any doubt (p-value smaller than 2.2e−16). Furthermore, assuming that the residuals are normally distributed, the Akaike information criterion:

$$\text{AIC} = 2k - 2\log(\tilde{\mathcal{L}})$$

with k the number of parameters (3 and 4 for the totally asymmetric and asymmetric models, respectively) and $\tilde{\mathcal{L}}$ the maximum likelihood, is much smaller for the asymmetric model (AIC = −9632.5) than for the initial totally asymmetric model (AIC = −5732). This confirms the enhancements of the new model even by taking into account that it includes one more parameter. Therefore, the improvements gained with the new parameter of the asymmetric model are statistically significant.

Finally, note that our observations are extracted from the trajectories and are time-dependent. The generalized least squares estimates, taking into account the (linear) time dependence, are close to the ordinary least squares estimates.

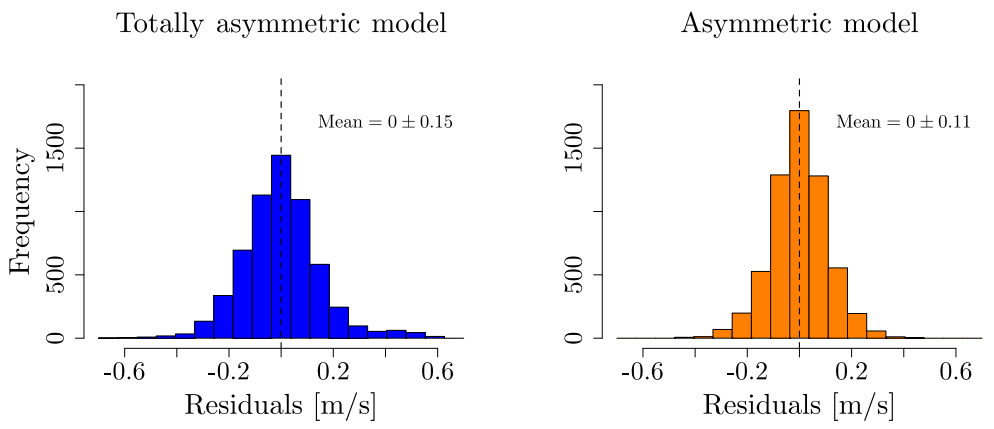

Fig. 6. Histograms of the residuals for the totally asymmetric model (left panel) and the asymmetric model (right panel). The distribution for the asymmetric model is slightly more concentrated.

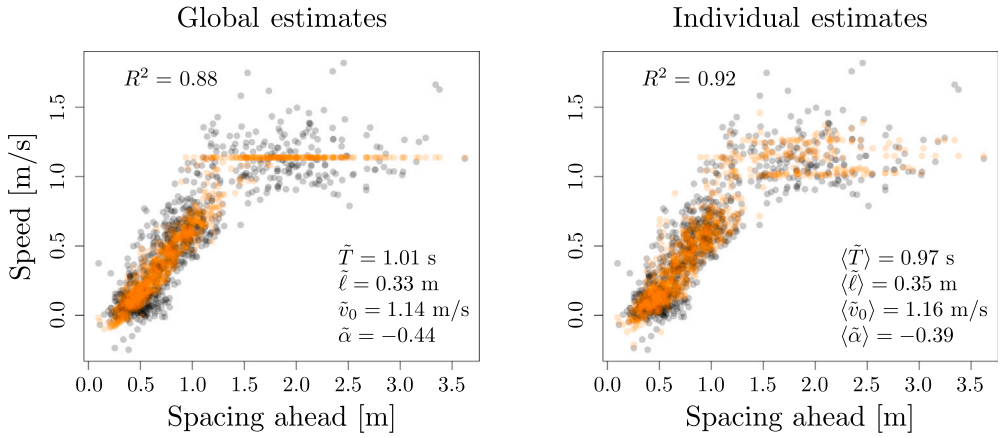

Fig. 7. Global (left panel) and individual (right panel) least squares estimates of the parameters using the CroMa dataset. The values for individual estimates are the averages for all the pedestrians. The parameter estimates are relatively stable. Note that only 16% of the observations and predictions are presented to improve the readability.

5.2.2. *Individual parameter estimates*

The CroMa experimental sample offers the possibility to identify the pedestrians in each experimental run. This allows the model parameters to be estimated individually for each pedestrian across all density levels. The estimates for the parameters (T, ℓ, v_0) of the optimal velocity function are close to those obtained using the BaSiGo dataset (see Fig. 7). The legend in the right panel gives the mean values over all estimates of pedestrians' individual parameters.

The histograms of the individual parameter estimates are depicted in Fig. 8. The variation ranges for parameter estimates of the optimal velocity function are reasonable. For the desired time gap $\tilde{T}$ the values range from 0.6 to 1.6 s. While for the pedestrian size $\tilde{\ell}$ the value ranges from 0.2 to 0.5 m, and for the desired speed $\tilde{v}_0$ from 0.9 to 1.6 m/s. Drawing attention to intriguing findings, that the individual estimates for the parameter α are systematically non-positive and may even be smaller than the critical stability threshold $\alpha_C = -1/2$.

A summary of the different estimates for the parameters of the totally asymmetric and asymmetric models is given in Table 2. It is noteworthy that the estimates are very similar for the different datasets (BaSiGo and CroMa) and estimation methods (global and individual). The parameters' values of the optimal velocity function for both the totally asymmetric and asymmetric models are approximately similar. These results confirm the accuracy of the estimates obtained and the characteristic behavior of single-file pedestrian motion.

5.2.3. *Remarks on estimation of α*

The estimates for the asymmetry parameter α are systematically negative and close to the critical stability value $\alpha_C = -1/2$ (see (13)). However, simulation results show that positive values for α, typically $\alpha = 1$, provide more realistic dynamics, especially regarding pedestrian overlap and backward movement when stop-and-go waves arise.

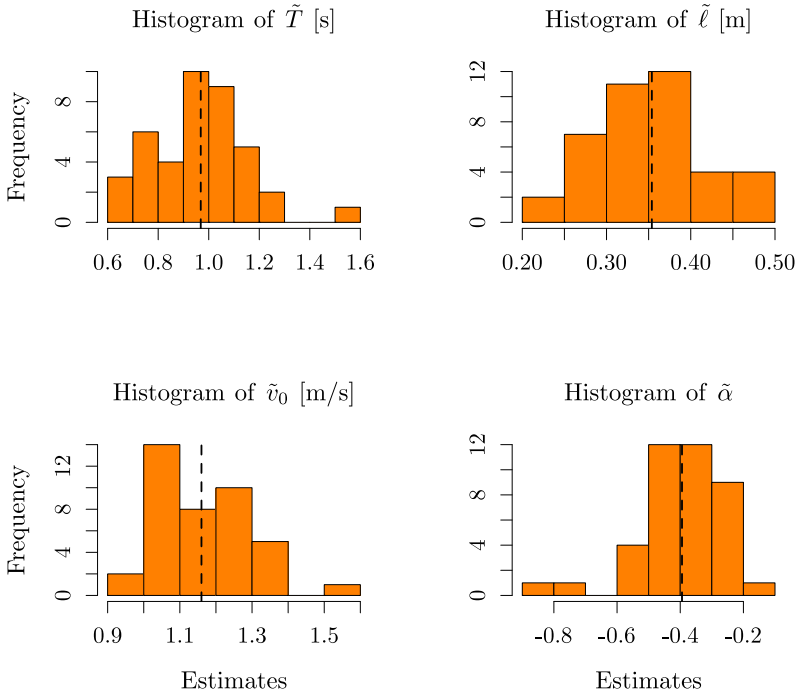

Fig. 8. Histograms of the parameter estimates by individual nonlinear least squares using the CroMa dataset.

Table 2
Table summarizing the statistical estimates of the models' parameters for global/individual estimates, totally asymmetric, and proposed models. The values for the individual estimates have the form $X \pm Y$ with X the mean value and Y the empirical standard deviation over all the individual pedestrian estimates. The parameter estimates are close to each other whatever the sample and method used. The AIC is calculated over an identical sample size of 6000 observations.

	Global estimates			Individual estimates
	BaSiGo dataset		CroMa dataset	
	Totally asym. model ($\alpha = 0$)	Asymmetric model (estimated α)		
$\tilde{T}$ [s]	1.04	0.98	1.01	0.97 ± 0.18
$\tilde{\ell}$ [m]	0.32	0.34	0.33	0.35 ± 0.06
$\tilde{v}_0$ [m/s]	1.19	1.19	1.14	1.16 ± 0.13
$\tilde{\alpha}$	–	−0.46	−0.44	-0.39 ± 0.14
R^2	0.86	0.93	0.88	0.92
AIC	−5732	−9632.5	−6123.4	−8722.7

In fact, the low estimates for α mainly result from simple kinematic effects to single file motion, regardless of the dynamical model. Assuming that the OV function $F : s \mapsto F(s) = s/T$ is linear, the cost function in the least squares estimates reads for the parameter α:

$$f(\alpha) = \sum_{k=1}^{K} \Big(v_k - \frac{1}{\tilde{T}} \big(\Delta x_k + \alpha (\Delta x_k - \Delta x_k^0) \big) \Big)^2 \tag{19}$$

and the derivative is given by:

$$f'(\alpha) = \frac{-2}{\tilde{T}} \sum_{k=1}^{K} (\Delta x_k - \Delta x_k^0) \Big(v_k - \frac{1}{\tilde{T}} \big(\Delta x_k + \alpha (\Delta x_k - \Delta x_k^0) \big) \Big). \tag{20}$$

The function f being convex, it is minimal if:

$$f'(\tilde{\alpha}) = 0 \quad \Leftrightarrow \quad \tilde{\alpha} = \frac{\sum_{k=1}^{K}(\Delta x_k - \Delta x_k^0)(v_k\tilde{T} - \Delta x_k)}{\sum_{k=1}^{K}(\Delta x_k - \Delta x_k^0)^2}. \tag{21}$$

The probabilistic distribution of the distances ahead and behind can reasonably be assumed to be identical. Assuming further that these distances and the speed are statistically independent, i.e., that there is no relationship between speed and distances, we asymptotically obtain:

$$\tilde{\alpha} \to -1/2 \qquad \text{as} \qquad K \to \infty, \tag{22}$$

since:

$$\frac{\sum_{k=1}^{K}(\Delta x_k - \Delta x_k^0)v_k\tilde{T}}{\sum_{k=1}^{K}(\Delta x_k - \Delta x_k^0)^2} \to 0, \tag{23}$$

while:

$$-\frac{\sum_{k=1}^{K}(\Delta x_k - \Delta x_k^0)\Delta x_k}{\sum_{k=1}^{K}(\Delta x_k - \Delta x_k^0)^2} = \frac{-\sum_{k=1}^{K}\Delta x_k^2 - \Delta x_k\Delta x_k^0}{\sum_{k=1}^{K}\Delta x_k^2 + (\Delta x_k^0)^2 - 2\Delta x_k\Delta x_k^0} \to -1/2, \tag{24}$$

as $K \to \infty$. The kinematic relationships of the single-file motion dominate and bring the statistical estimate for α close to the critical stability condition for which the model is symmetric. The fine-tuning effects of the asymmetric mechanisms weighted by α occur at a lower level, through the interdependence between the distances and the speed. Therefore, the statistical estimate of the asymmetry parameter α is strongly influenced by the kinematic relationship of the single-file movement. This can lead to misleading calibration values for this parameter. In the following simulation analysis, we manually calibrate α and observe that positive values, e.g., $\alpha = 1$, give more realistic dynamics.

6. Simulation results

6.1. Simulation setup

We numerically simulate the asymmetric single-file pedestrian model using an Euler–Maruyama scheme. The numerical solver reads:

$$\begin{cases} x_n(t+\delta t) = x_n(t) + \delta t F\big(\Delta x_n(t) + \alpha(\Delta x_n(t) - \Delta x_{n-1}(t))\big) + \delta t\xi_n(t), \\ \xi_n(t+dt) = \xi_n(t)(1-\delta t\gamma) + \sqrt{\delta t}\sigma Z_n(t), \end{cases} \tag{25}$$

with the time step $\delta t = 0.01$ s and independent normal random variables $(Z_n(t),\ t = m\delta t,\ m \in \{0,1,2,\dots\})_n$. Here F is the smoothed OV function given in Eq. (4) with $v_0 = 1.19$ m/s, $T = 0.98$ s and $\ell = 0.34$ m. The speed smoothing is equal to $\varepsilon = 0.01$ m/s. For the noise parameters, we use the same estimates as [2] in the simulation, namely $\sigma = 0.09\ \text{ms}^{-3/2}$ and $\gamma = 0.23\ \text{s}^{-1}$. The values for α will be set manually, ranging from -0.25 to 2. The size of the geometry and number of pedestrians are set as in the BaSiGo and CroMa experiences. The initial condition is uniform with speeds zero.

6.2. Assessing the asymmetry parameter by simulation

We assess the asymmetry parameter α by estimating the parameters using synthetic datasets obtained by simulation. The aim is to evaluate how strong the influence of the kinematic single-file relationships on the least squares estimates for α. The scatter plots of real and synthetic data with corresponding least squares parameter estimates are shown in Fig. 9 and Table 3.

We can clearly observe in the figure that decreasing α increases the scattering of the data points. The simulation with $\tilde{\alpha} = -0.46$ as statistically estimated, shows an unrealistically larger scatter.

As expected, the least squares estimates for the asymmetry parameter α remain constant, close to the critical stability condition $\alpha_C = -1/2$. This holds even when $\alpha >> 0$ in the model, confirming the predominance of the kinematic single-file relationships in the dynamics and the limited significance of the statistical estimates. The estimates of the parameter (T, ℓ, v_0) of the OV function (4) are also stable. Only the estimates for the desired speed v_0 slightly decrease as α increases due to the nonlinear shape of the OV function.

6.3. Main simulation results

In this section, we compare the real data of the BaSiGo experiment with the simulation results of the totally asymmetric model and the new asymmetric model. The parameters of the deterministic speed models are set as follows: the desired speed is $v_0 = 1.19$ m/s, the desired time gap is $T = 0.98$ s, the pedestrian size is $\ell = 0.34$ m, while the noise parameters are equal to $\sigma = 0.09\ \text{ms}^{-3/2}$ and $\gamma = 0.23\ \text{s}^{-1}$. The dimensionless asymmetry parameter α is set to zero for the totally asymmetric model whereas it is equal to one for the new asymmetric model. Several simulation runs are carried out with different numbers of pedestrians $N = 15$, 30, 47, 52, 55, and 59 as in the BaSiGo experiment.

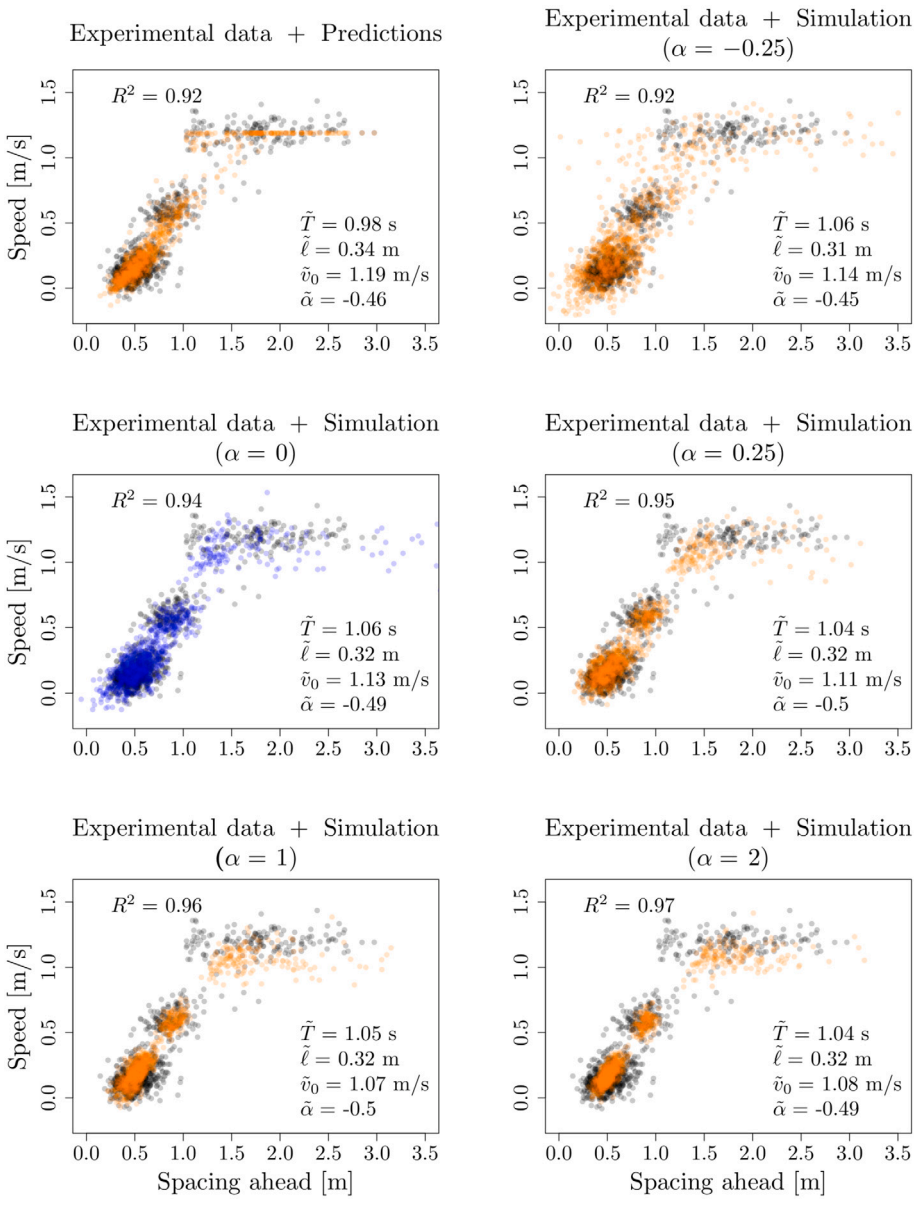

Fig. 9. Least squares parameter estimates and pedestrian distance-speed scatter plots for the BaSiGo experiment (gray dots), the model prediction (upper left plot), and simulation results for α between -0.25 and 2 (remaining plots). The estimates for the asymmetry parameter α remain constant, close to the critical stability condition $\alpha_C = -1/2$, even for the synthetic data when $\alpha >> 0$. Note that only 16% of data points are presented.

6.3.1. Fundamental diagram

We compare the fundamental relationship between the distance ahead and the speed, as well as the distributions of the speed and distance individually (see Fig. 10). It is noteworthy that the asymmetric model better shapes the data point scatter of the fundamental diagram compared to the totally asymmetric model (see Fig. 10, upper panels). In both real and synthetic data obtained with the asymmetric model, three main clusters can be observed. These clusters are also present in the totally asymmetric model, but they are less pronounced.

The marginal distributions of the speed and distance confirm the improvements obtained with the asymmetric interaction model. Regarding the speed distribution, both the real data and simulation results from the new model exhibit close similarities, with three modes of identical amplitude. Conversely, the shape of the three modes is less pronounced in the totally asymmetric model (see Fig. 10, middle panels). As for the distance distributions, they appear relatively compact and similar for the real data and the asymmetric model, with distances less than 3 and 4 m, respectively. In contrast, the totally asymmetric model distance distributions have an unrealistically large tail with distances up to 8 meters (see Fig. 10, bottom panels). Furthermore, both the real data and

Table 3
Table summarizing the estimates of the model's parameters by nonlinear least squares using the BaSiGo data set and synthetic data obtained by simulation with α ranging between −0.25 and 2. The symbols $\tilde{T}$, $\tilde{\ell}$, $\tilde{v}_0$, and $\tilde{\alpha}$ are the parameter values estimated by least squares. Note that although the setting for α ranges from −0.25 to 2 in the simulations, the estimates remain stable around −0.5 due to kinematic single-file effects.

	BaSiGo	Synthetic data				
		$\alpha = -0.25$	$\alpha = 0$	$\alpha = 0.25$	$\alpha = 1$	$\alpha = 2$
$\tilde{T}$ [s]	0.98	1.06	1.06	1.04	1.05	1.04
$\tilde{\ell}$ [m]	0.34	0.31	0.32	0.32	0.32	0.32
$\tilde{v}_0$ [m/s]	1.19	1.14	1.13	1.11	1.07	1.08
$\tilde{\alpha}$	−0.46	−0.45	−0.49	−0.5	−0.5	−0.49
R^2	0.92	0.92	0.94	0.95	0.96	0.97

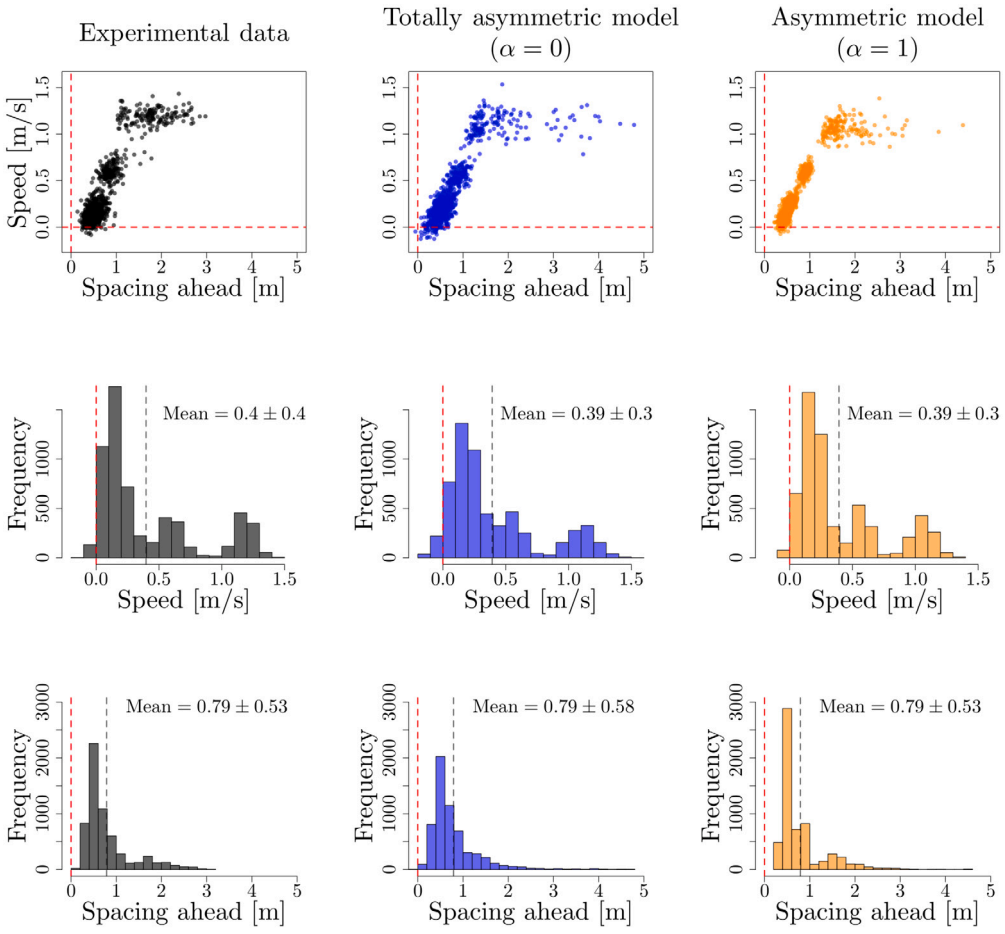

Fig. 10. Distance-speed scatterplot (upper panels), speed histogram (middle panels) and spacing ahead histogram (bottom panels) of BaSiGo experimental data (left panel) and the simulation results of totally asymmetric ($\alpha = 0$, central panels) and asymmetric ($\alpha = 1$, right panels) models for runs $N = 15, 30, 47, 52, 55, 59$. Note that only 16% of the data samples were used in the scatter plots. The red dashed line is located on zero to indicate the negative values of the speed and distance ahead.

the simulation results from the asymmetric model show a minimal occurrence of negative values for speed and distance compared to the totally asymmetric model (see the left tail of the distributions in Fig. 10, middle and lower panels).

6.3.2. *Space–time diagram*

In this section, we compare the real (BaSiGo experiment) and synthetic single-file trajectories obtained from the totally asymmetric and asymmetric models with 59 participants (see Fig. 11).

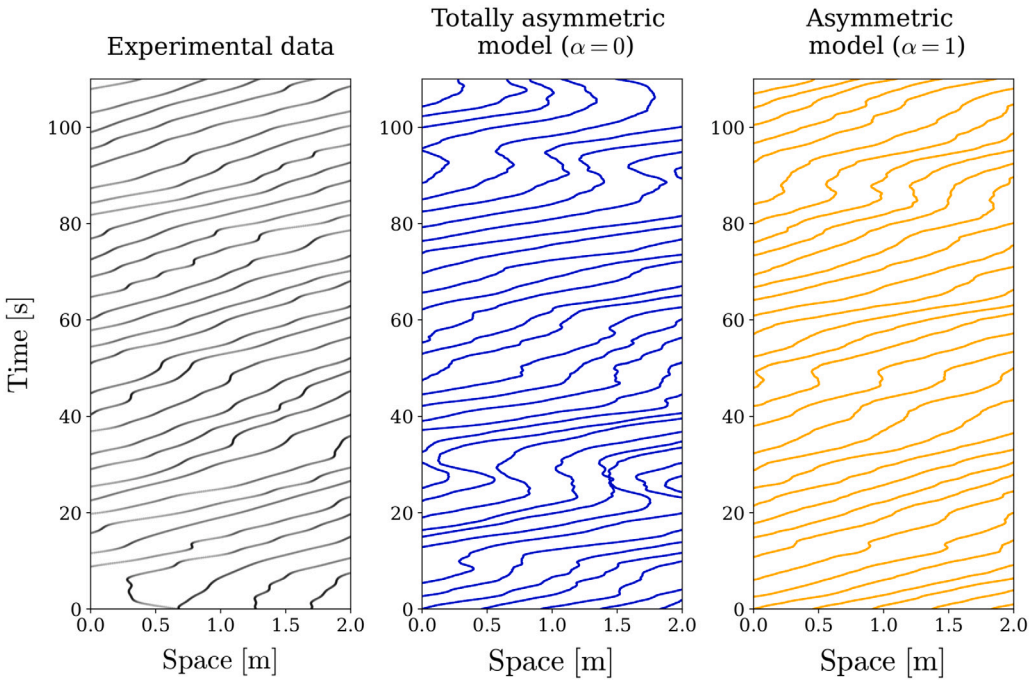

Fig. 11. Trajectories of $N = 59$ pedestrian walking on a ring of length 27 m observed over a segment of length 2 m. From left to right: real data (BaSiGo experiment), totally asymmetric model ($\alpha = 0$), and asymmetric model ($\alpha = 1$), respectively.

It is observed that the totally asymmetric model shows more backward movement with negative speed and overlap compared to the real data. This aligns with the previously mentioned findings regarding the left tail of the speed and distance distributions, which spread out in the totally asymmetric model (refer to Fig. 10, middle and bottom panels). The simulations for the asymmetric model with $\alpha = 1$ show fewer backward movements, making the stop-and-go waves qualitatively more realistic. This improvement is obvious in the crowded experiment with 59 participants.

Another enhancement introduced by our proposed model is to make the noise parameters constant. In previous work [2], the noise parameters (σ and γ) are state-dependent, meaning that multiple values for the noise parameters (σ or γ) are estimated depending on the distance class (refer to Fig. 7 in the paper [2]). By introducing the distance to the follower, we simplify the calibration process for the noise parameters, making the calculations much easier.

7. Conclusions

We present an original asymmetric stochastic model describing the movement of pedestrians in one-dimensional space (single-file motion). Taking inspiration from statistical analysis [22] and observation of coordination in pedestrian single-file motion [23], we include the distance to the follower in the OV model, resulting in an asymmetric interaction model including a fine-tuning asymmetry parameter α. Statistical estimates of the model using experimental data enable parameter calibration and interpretation. They also demonstrate that the enhancement brought by the new parameter is statistically significant. The comparison of the experimental data and synthetic data of the improved model under different settings of α, specifically $\alpha = 0$ and $\alpha = 1$, shows a strong agreement between the asymmetric model results and the experimental data. The simulations performed with positive α exhibit reduced backward movements, resulting in stop-and-go waves that closely resemble the experimental data. Additionally, the model describes a realistic fundamental diagram and, in particular, its scattering. Further evaluation in terms of validation and verification to assess the model's overall performance will be undertaken in future work. The proposed model should also be benchmarked against various models found in the literature.

CRediT authorship contribution statement

Rudina Subaih: Conceptualization, Methodology, Software, Validation, Formal analysis, Investigation, Data curation, Writing – original draft, Writing – review & editing. **Antoine Tordeux:** Conceptualization, Methodology, Software, Validation, Formal analysis, Investigation, Writing – review & editing, Supervision.

Declaration of competing interest

We wish to confirm that there are no known conflicts of interest associated with this publication. This work was supported by the German Federal Ministry of Education and Research (BMBF: funding number 01DH16027) within the framework of the Palestinian-German Science Bridge project.

Data availability

Data will be made available on request.

Acknowledgment

This work was supported by the German Federal Ministry of Education and Research (BMBF: funding number 01DH16027) within the framework of the Palestinian-German Science Bridge project. All authors have read and agreed to the published version of the manuscript.

References

[1] J. Cordes, M. Chraibi, A. Tordeux, A. Schadschneider, Time-to-collision models for single-file pedestrian motion, Collect. Dyn. 6 (2021) 1–10.
[2] A. Tordeux, A. Schadschneider, White and relaxed noises in optimal velocity models for pedestrian flow with stop-and-go waves, J. Phys. A 49 (18) (2016) 185101.
[3] M. Chraibi, T. Ezaki, A. Tordeux, K. Nishinari, A. Schadschneider, A. Seyfried, Jamming transitions in force-based models for pedestrian dynamics, Phys. Rev. E 92 (4) (2015) 042809.
[4] S. Lemercier, A. Jelic, R. Kulpa, J. Hua, J. Fehrenbach, P. Degond, C. Appert-Rolland, S. Donikian, J. Pettré, Realistic following behaviors for crowd simulation, in: Computer Graphics Forum, Vol. 31, Wiley Online Library, 2012, pp. 489–498.
[5] H. Kuang, Y. Fan, X. Li, L. Kong, Asymmetric effect and stop-and-go waves on single-file pedestrian dynamics, Procedia Eng. 31 (2012) 1060–1065.
[6] A. Portz, A. Seyfried, Analyzing stop-and-go waves by experiment and modeling, in: Pedestrian and Evacuation Dynamics, Springer, 2011, pp. 577–586.
[7] M. Chraibi, A. Seyfried, A. Schadschneider, Generalized centrifugal-force model for pedestrian dynamics, Phys. Rev. E 82 (4) (2010) 046111.
[8] T. Kretz, On oscillations in the social force model, Physica A 438 (2015) 272–285.
[9] I. Karamouzas, B. Skinner, S.J. Guy, Universal power law governing pedestrian interactions, Phys. Rev. Lett. 113 (23) (2014) 238701.
[10] A. Tordeux, M. Chraibi, A. Seyfried, Collision-free speed model for pedestrian dynamics, in: Traffic and Granular Flow'15, Springer, 2016, pp. 225–232.
[11] J. Ondřej, J. Pettré, A.-H. Olivier, S. Donikian, A synthetic-vision based steering approach for crowd simulation, ACM Trans. Graph. 29 (4) (2010) 1–9.
[12] A. Schadschneider, Cellular automaton approach to pedestrian dynamics-theory, in: M. Schreckenberg, S. Sharma (Eds.), Pedestrian and Evacuation Dynamics, Springer, Berlin/Heidelberg, 2001, pp. 75–86.
[13] D. Helbing, P. Molnar, Social force model for pedestrian dynamics, Phys. Rev. E 51 (5) (1995) 4282.
[14] K. Hirai, K. Tarui, A simulation of the behavior of a crowd in panic, in: Proc. of the 1975 International Conference on Cybernetics and Society, San Francisco, 1975, pp. 409–411.
[15] N. Bellomo, B. Piccoli, A. Tosin, Modeling crowd dynamics from a complex system viewpoint, Math. Models Methods Appl. Sci. 22 (supp02) (2012) 1230004.
[16] R.L. Hughes, A continuum theory for the flow of pedestrians, Transp. Res. B 36 (6) (2002) 507–535.
[17] R.L. Hughes, The flow of human crowds, Annu. Rev. Fluid Mech. 35 (1) (2003) 169–182.
[18] R. Hughes, The flow of large crowds of pedestrians, Math. Comput. Simulation 53 (4–6) (2000) 367–370.
[19] D. Helbing, A fluid dynamic model for the movement of pedestrians, 1998, arXiv preprint cond-mat/9805213.
[20] L.F. Henderson, On the fluid mechanics of human crowd motion, Transp. Res. 8 (6) (1974) 509–515.
[21] M. Chraibi, A. Tordeux, A. Schadschneider, A. Seyfried, Modelling of pedestrian and evacuation dynamics, Encycl. Complex. Syst. Sci. (2018) 1–22.
[22] R. Subaih, M. Maree, A. Tordeux, M. Chraibi, Questioning the anisotropy of pedestrian dynamics: An empirical analysis with artificial neural networks, Appl. Sci. 12 (15) (2022) 7563.
[23] K.W. Rio, C.K. Rhea, W.H. Warren, Follow the leader: Visual control of speed in pedestrian following, J. Vision 14 (2) (2014) 4.
[24] S. Paetzke, M. Boltes, A. Seyfried, Influence of gender composition in pedestrian single-file experiments, 2023, arXiv preprint arXiv:2302.11168.
[25] R. Subaih, M. Maree, M. Chraibi, S. Awad, T. Zanoon, Experimental investigation on the alleged gender-differences in pedestrian dynamics: A study reveals no gender differences in pedestrian movement behavior, IEEE Access 8 (2020) 33748–33757.
[26] A. Fujita, C. Feliciani, D. Yanagisawa, K. Nishinari, Traffic flow in a crowd of pedestrians walking at different speeds, Phys. Rev. E 99 (6) (2019) 062307.
[27] A. Aw, A. Klar, M. Rascle, T. Materne, Derivation of continuum traffic flow models from microscopic follow-the-leader models, SIAM J. Appl. Math. 63 (1) (2002) 259–278.
[28] M. Chraibi, U. Kemloh, A. Schadschneider, A. Seyfried, Force-based models of pedestrian dynamics, Netw. Heterog. Media 6 (3) (2011) 425.
[29] M. Chraibi, Oscillating behavior within the social force model, 2014, arXiv preprint arXiv:1412.1133.
[30] J. Cordes, A. Schadschneider, A. Tordeux, The trouble with 2nd order models or how to generate stop-and-go traffic in a 1st order model, in: Traffic and Granular Flow 2019, Springer, 2020, pp. 45–51.
[31] I.M. Sticco, G.A. Frank, F.E. Cornes, C.O. Dorso, A re-examination of the role of friction in the original social force model, Saf. Sci. 121 (2020) 42–53.
[32] A. Tordeux, A. Seyfried, Collision-free nonuniform dynamics within continuous optimal velocity models, Phys. Rev. E 90 (4) (2014) 042812.
[33] M. Ma, W. Wang, S. Liang, J. Xiao, C. Wu, Improved car-following model for connected vehicles considering backward-looking effect and motion information of multiple vehicles, J. Transp. Eng. A Syst. 149 (2) (2023) 04022148.
[34] D. Ma, Y. Han, F. Qu, S. Jin, Modeling and analysis of car-following behavior considering backward-looking effect, Chin. Phys. B 30 (3) (2021) 034501.
[35] G. Ma, M. Ma, S. Liang, Y. Wang, H. Guo, Nonlinear analysis of the car-following model considering headway changes with memory and backward-looking effect, Physica A 562 (2021) 125303.
[36] D. Yang, P. Jin, Y. Pu, B. Ran, Safe distance car-following model including backward-looking and its stability analysis, Eur. Phys. J. B 86 (2013) 1–11.
[37] H. Ge, H. Zhu, S. Dai, Effect of looking backward on traffic flow in a cooperative driving car the following model, Eur. Phys. J. B 54 (2006) 503–507.
[38] A. Nakayama, Y. Sugiyama, K. Hasebe, Effect of looking at the car that follows in an optimal velocity model of traffic flow, Phys. Rev. E 65 (1) (2001) 016112.
[39] J. Monteil, R. Billot, J. Sau, N.-E. El Faouzi, Linear and weakly nonlinear stability analyses of cooperative car-following models, IEEE Trans. Intell. Transp. Syst. 15 (5) (2014) 2001–2013.
[40] F. Nielsen, K. Sun, Guaranteed bounds on information-theoretic measures of univariate mixtures using piecewise log-sum-exp inequalities, Entropy 18 (12) (2016) 442.
[41] V. Ziemer, A. Seyfried, A. Schadschneider, Congestion dynamics in pedestrian single-file motion, in: Traffic and Granular Flow'15, Springer, 2016, pp. 89–96.